Stiffness and Damping Formulations for Jointed Deployable Space Truss Structure

A Xi[1] **W Zhang**[1] **and Gen Liu**[1]

[1] College of Mechanical Engineering, Beijing University of Technology, Beijing, 100124, PR China

xiansu30@126.com

Abstract. In this paper, the dynamic behaviors of a elastic rod connected by a joint with clearance of deployable truss structures are investigated. A one-dimensional cantilever with joint support is examined in the deployable truss structure. These formulations consist of the nonlinear joint dynamic stiffness model and damping models are formulated and the dynamic characteristics of free-vibrating structures are estimated. The natural frequency transitions are investigated by considering the contact and noncontact conditions of the clearances, then the formulation of dynamic stiffness model is obtained. The friction models are mathematically formulated and simplified to make them easy to calculate. The impact damping models are formulated using the linear envelope of the time response and it can be negligible when the speed is small. The dynamic characteristics can be estimated by integrating these models and formulations using the energy loss factors. Experimental evaluations show the dynamic characteristics and demonstrate the validity of the formulations.

1. Introduction

The deployable space structures have characteristics of large size high precision [1-4]. The deployable structures not only satisfy the mission requirement but also to meet the good mechanical properties. With the characteristics of light weight, high storage ratio and enough stiffness, the truss become the preferred deployable structures[5,6]. The ring truss structure in the deployable antenna often need the hinge to connect each other, however, the hinge gap is inevitable. The gaps in the hinge make the truss structure to show a complex dynamic behaviour[7,8]. Therefore, it is important to study the characteristics of the joints in the ring truss support structure.

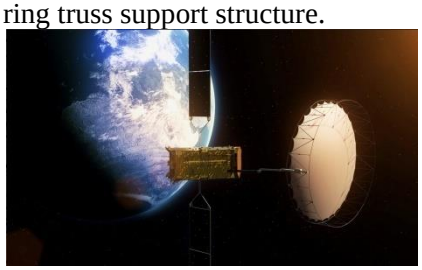

Figure 1. Truss antenna reflector.

In the research of hinge structure, scholars have done a lot of work. Hu et al. [9] put forward three scientific problems on the nonlinear dynamics and control of the large ring truss reflector structure. The effective of gaps in the nonlinear joint is studied. Yoshida [10] study the clearance hinge in the

space structure, and the mechanical model of the hinge is established. Wang et al. [11] study on the nonlinear dynamic problems of two - bar structures with clearances. Lion et al. [12,13] uses the amplitude frequency response function to identify the dynamic parameters of the hinge. Crawley et al. [14-17] applies force state mapping method (FSM) to the parameter identification of nonlinear hinge, and uses the method to identify the model and parameters of spacecraft joint structure. The time history of the restoring force and the time history of the state variables are measured, and the least square method is used to fit the relationship between the restoring force and the state variable.

Stiffness and damping are important factor in determining the dynamic characteristics of hinge structure, this paper will analyze the radial dynamic characteristics of the planar revolute hinge on the connection of deployable ring truss antenna structure. The radial dynamic model of the hinge is established, and the dynamic stiffness and damping of the hinge are analyzed. Meanwhile, the relevant dynamic model is verified by experiments.

2. Radial dynamic stiffness of hinge

The ring truss deployable antenna is composed of a large number of bars and joints, and the whole structure is divided into mesh, the front net, ring truss tension ties and rear net, as shown in Figure2. The ring truss is the frame of the antenna, which plays a role in supporting surface and keeps the antenna structure stable.

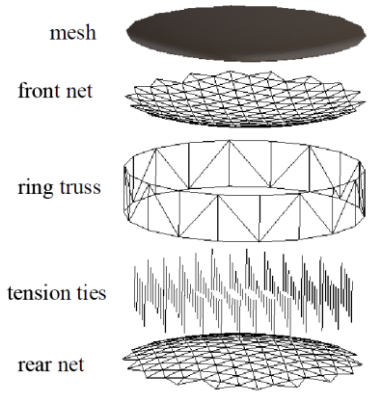

Figure 2. Sketch of circular truss

The stiffness of the joint is an important factor to determine the dynamic characteristics of the jointed structure. The assembly of the hinge and the pin provides the condition for the existence of the gap, and the gap between the hinge and the pin is inevitable in the process of manufacture, assembly and transportation.

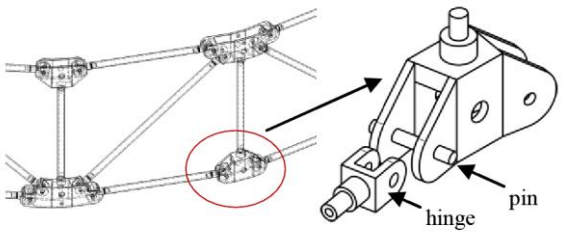

Figure 3. Sketch of rotary hinge

In this section, the radial dynamic characteristics of the planar revolute hinge in the annular truss antenna support structure are analyzed.

2.1. Static stiffness of hinge

Hertz contact theory is a theory of elastic non coordination of contact problems, the three-dimensional cylindrical contact is simplified to a two-dimensional contact, in Figure 4. The Hertz contact force

model is based on the complete elastic deformation, which mainly deals with the quasi-static contact problem of the elastic body, however, the energy loss during contact is not considered.

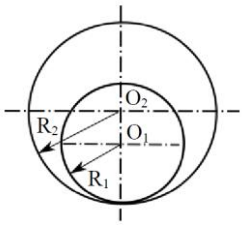

Figure 4. Contact state of rotary hinge

The Hertz contact force model is based on the complete elastic deformation, which mainly deals with the quasi-static contact problem of the elastic body, however, the energy loss during contact is not considered.

The Hertz contact force model can be described by a nonlinear spring

$$F_n = k_j \delta^n \tag{1}$$

where δ is the elastic deformation, k_j is the contact stiffness coefficient, the expression is as follows:

$$\mathrm{k_j} = \frac{4}{3\pi\left(\sigma_i + \sigma_j\right)}\left[\frac{R_1 R_2}{R_2 - R_1}\right]^{\frac{1}{2}} \tag{2}$$

where, σ_i , σ_j are contact modulus. $\frac{R_1 R_2}{R_2 - R_1}$ is the equivalent radius of contact.

$$\sigma_i = \frac{1-\upsilon_i^2}{\pi E_i}, \sigma_j = \frac{1-\upsilon_j^2}{\pi E_j} \tag{3}$$

The static stiffness is the relative stiffness at the moment of contact between the hinge and the pin.

2.2. Dynamic stiffness of hinge

The stiffness of the hinge under external excitation is studied, it is necessary to establish the dynamic stiffness model of clearance hinge. The natural frequency and dynamic stiffness of the hinge is derived. In figure 5, the motion of the clearance hinge can be divided into three states: gap state, transition state and contact state.

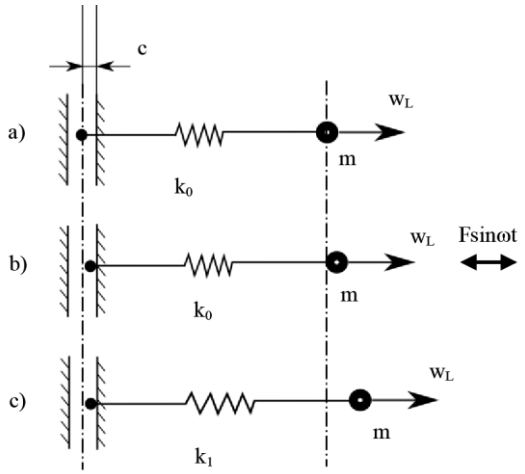

Figure 5. a) Gap state. b) Transition state. c) Contact state

In the contact and noncontact conditions, the equations of motion for the equivalent systems are given as

$$m\ddot{w}_L + k_0 w_L = 0 \quad (w_L \le \varepsilon) \tag{4}$$

$$m\ddot{w}_L + k_1 w_L = (k_1 - k_0)\varepsilon \quad (w_L > \varepsilon) \tag{5}$$

where $\ddot{w}_L$ is the acceleration of m, w_L is the deflection of m.

In the state, the displacement of the mass can be set

$$w_L = C_1 \sin \omega_0 t + C_2 \cos \omega_0 t \tag{6}$$

where C_1, C_2 are coefficient related to initial condition. ω_0 is the circular frequency of the hinge in the gap state. The initial condition of the hinge motion is assumed to be $t = 0$, $w_L = 0$, $\dot{w}_L = v_0$, $C_1 = v_0 / \omega_0$, $C_2 = 0$. When the hinge is in the transition state, according to the displacement continuity condition, $t = t_1$, $x = c$. Moreover, according to the law of conservation of energy, when the vibration displacement peak value is A, the potential energy is equal to the kinetic energy of the initial system

$$mv_0^2 / 2 = k_1 A^2 / 2 \tag{7}$$

The duration of the gap state is calculated

$$t_1 = \frac{1}{\omega_0} \arcsin \frac{\omega_0 c}{\omega_1 A} \tag{8}$$

where ω_1 is circular frequency of the contact state,

$$\omega_1 = \sqrt{\frac{k_1}{m}} \tag{9}$$

The duration of the contact state is

$$t_2 = \frac{1}{\omega_1} \arccos \frac{c}{c + A\lambda^2} \tag{10}$$

where λ is the natural frequency ratio of contact state and gap motion state.

$$\lambda = \frac{\omega_1}{\omega_0} \tag{11}$$

According to the literature [15], the natural frequency of the gap hinge structure is obtained by the superposition of the contact state and the gap state

$$f = \frac{1}{4}\left(\frac{1}{\omega_0} \arcsin \frac{\omega_0 c}{\omega_1 A} + \frac{1}{\omega_1} \arccos \frac{c}{c + A\lambda^2} \right)^{-1} \tag{12}$$

In the process of the radial movement of the hinge, when the hinge is in the gap state, $k_0 = 0$, and the natural frequency of the hinge can be expressed as

$$f = \frac{1}{4} \lim_{\omega_0 \to 0} \left(\frac{1}{\omega_0} \arcsin \frac{\omega_0 c}{\omega_1 A} + \frac{1}{\omega_1} \arccos \frac{c}{c + A\lambda^2} \right)^{-1} \tag{13}$$

$$f = \frac{\omega_1}{2\pi} \left(\frac{2c}{\pi A} + 1 \right)^{-1} \tag{14}$$

By Eq.14, the natural frequency of the hinge structure is directly proportional to the natural frequency of the contact section, meanwhile, the increase of the gap leads to the decrease of the natural frequency of the structure, furthermore, the natural frequency increases with the increase of amplitude.

The amplitude under external excitation is

$$w_{\max} = \frac{F / k}{\sqrt{[1 - (\omega / \omega_n)^2] + [2\zeta(\omega / \omega_n)]^2}} \tag{15}$$

where the circular frequency of the gap hinge structure is ω_n, k is static stiffness, ω is the circular frequency of external excitation, ζ is damping ratio. By Ref. [16], because the ζ is small, when the

exciting force is small, the denominator of Eq.15 is simplified, and the dynamic stiffness k_d is obtained

$$k_d = kc_d = k\left|1-\left(\frac{\omega}{\omega_n}\right)^2\right| = k\left|1-[\frac{\omega}{\omega_1}\left(\frac{2c}{\pi A}+1\right)]^2\right| \tag{16}$$

Can be obtained by Eq.16, the dynamic stiffness coefficient changes with the natural frequency and the external excitation frequency of the gap hinge structure as well as the dynamic stiffness coefficient changes with the gap size and amplitude. Figure6 and Figure7 show the trend of dynamic stiffness coefficient. The dynamic stiffness can be seen from the chart, the influence of the gap size on the dynamic stiffness coefficient is significant.

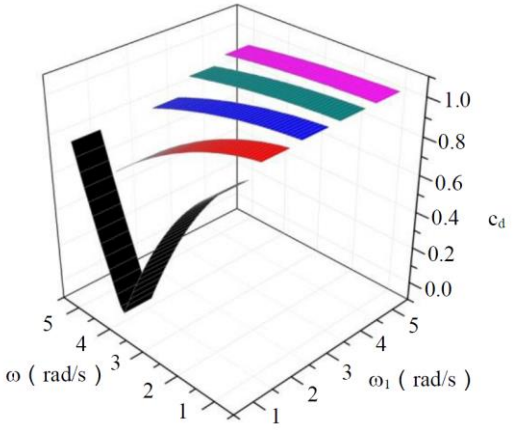

Figure 6. The trend of dynamic stiffness coefficient varying with frequency

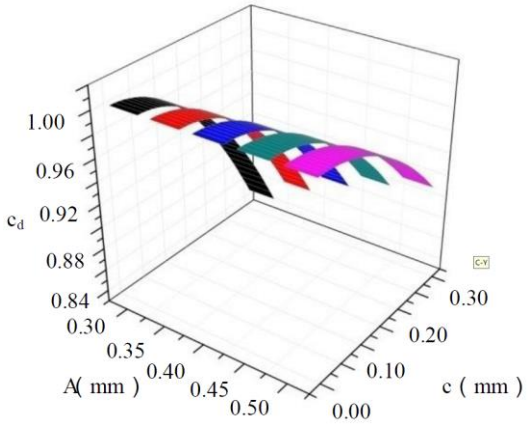

Figure 7. The trend of dynamic stiffness coefficient varying with amplitude and gap

3. Energy dissipation of the joint

The radial clearance of the pin-joint leads to the friction and impact when the vibration occurs. In order to model the joint damping in the hinge structure, it is necessary to analyze the radial energy dissipation.

The assembly error leads to the existence of sliding friction on the side of the hinge, and the energy dissipation caused by the sliding friction under the action of the F_p :

$$E_{slide} = \int_{t_1}^{t_2} c\dot{x}^2 dt = \int_{t_1}^{t_2} \frac{4\mu F_p}{\omega\pi A}\dot{x}^2 dt \tag{17}$$

where μ is the friction coefficient.

The friction force not only exists on the side of the hinge, but also occurs on the contact surface. The energy dissipation caused by contact friction can be obtained by analyzing the velocity of the contact surface. When the normal contact velocity is v, the contact half angle of the contact point is θ on the impact surface, the tangential velocity can be expressed in v_τ .

$$v_\tau = v\sin\theta \tag{18}$$

There are two contacts in the hinge in a period, so the energy dissipation caused by the contact friction is expressed as:

$$E_{conact} = 8\int_{t_1}^{t_2}\int_0^{\alpha}\mu N v\sin\theta d\theta dt \tag{19}$$

where N is the distributed contact force, α is the contact half angle, t_1 is the starting time of contact, t_2 is the termination time of contact.

Distributed contact force is:

$$N = \frac{E\sqrt{\delta-\theta^2 R}}{2\sqrt{R}} \tag{20}$$

where δ is contact depth, R is equivalent radius.

The velocity of the contact points in the contact area:

$$v = \frac{d\delta_w}{dt} = \frac{1}{2}\frac{\dot{\delta}\sqrt{\delta - \theta^2 R}}{\sqrt{\delta} + \sqrt{\delta}\sqrt{\delta - \theta^2 R}} \tag{21}$$

where $\delta_w = \sqrt{\delta}\sqrt{\delta - \theta^2 R}$.

The energy dissipation caused by contact friction can be expressed as:

$$E_{conact} = 8\int_{t_1}^{t_2}\int_0^{\alpha} \mu \frac{E\dot{\delta}}{4\sqrt{\delta R}}\left(2\delta - \theta^2 R\right)\sin\theta d\theta dt \tag{22}$$

The hinge clearance leads to the relative motion between the components, and when the two parts collide with each other the energy dissipated is

$$E_{impact} = \frac{1}{2}mv^2 \tag{23}$$

where v is velocity before impact.

Based on the above theory, the hinge radial energy dissipation produced by friction and impact can be expressed as:

$$E_{damp} = E_{slide} + E_{contact} + E_{impact} \tag{24}$$

The reduction of vibration caused by friction and collision can be measured by energy dissipation factor The energy dissipation factor is defined as the ratio of the energy dissipation to the total energy of a single cycle, so the energy dissipation factor D is:

$$D = \frac{E_{damp}}{E_{total}} \tag{25}$$

where E_{total} is total energy per cycle.

The relationship between the energy dissipation factor and the damping ratio is derived by combining the damping concept in the structural dynamics. The total energy of the structure at the beginning of deformation can be expressed as:

$$E_{total} = \frac{1}{2}ka_i^2 \tag{26}$$

where a_i is the displacement amplitude of periodic i , k is the stiffness of the structure. The energy dissipation expressed by displacement amplitude in a period is

$$E_{damp} = \frac{1}{2}k\left(a_i^2 - a_{i+1}^2\right) \tag{27}$$

Therefore, the energy dissipation factor can be expressed as

$$D = 1 - \left(\frac{a_{i+1}}{a_i}\right)^2 \tag{28}$$

The attenuation rate of structural vibration can be expressed as

$$\eta = \ln\frac{a_i}{a_{i+1}} = \ln(1 + \frac{a_i - a_{i+1}}{a_i}) \approx -1 + \frac{a_i}{a_{i+1}} \tag{29}$$

When the damping is small, the relationship between damping ratio η and energy dissipation factor D is obtained based on power series expansion

$$\xi = \frac{\eta}{2\pi} \approx \frac{0 + 1/2D}{2\pi} = \frac{E_{damp}}{4\pi E_{total}} \tag{30}$$

Therefore, the energy dissipation factor is proportional to the damping ratio, both of which can reflect the change of structural damping.

4. Radial dynamics experiment of the hinge

The dynamic experiment of the radial motion of the hinge structure is shown in Figure 8 and Figure 9. The external excitation of the hinge is sinusoidal, and laser sensor is used to acquire the displacement of hinge. The experimental part is the planar revolute hinge, the geometric dimensions as shown in Figure 10. The clearance is formed by matching the hinge size with the pin diameter, see table (1) for clearance data of hinge and column pin. Exert Sinusoidal excitation on the hinge, displacement of hinge radial vibration of will be acquired.

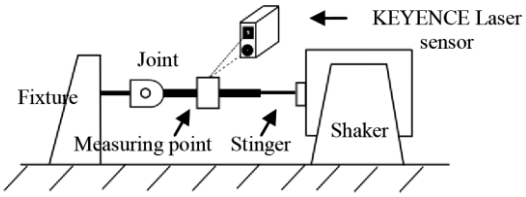

Figure 8. Experimental equipment layout

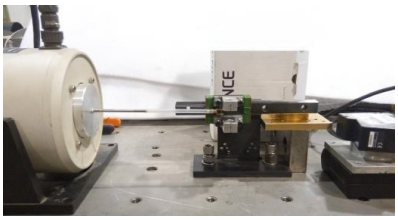

Figure 9. Experimental equipment

Table 1. Clearance value

R_2	R_1	c
3.0mm	2.1mm	0.45mm
	2.4mm	0.30mm
	2.5mm	0.25mm
3.2mm	2.1mm	0.55mm
	2.4mm	0.40mm
	2.5mm	0.35mm

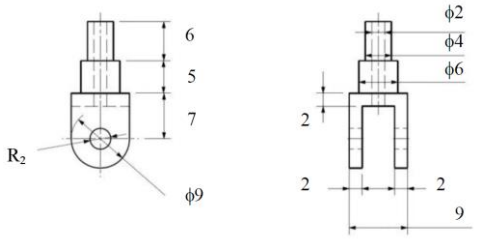

Figure 10. Geometry of hinge

When the excitation frequency is 5Hz, the clearance is 0.4mm, and the excitation amplitude is 0.604mm, the relationship between the external excitation amplitude and the hinge amplitude is shown in Figure11. From the chart, the external excitation is affected by the hinge motion and the amplitude is reduced; The time to reach the peak value of the hinge lags behind the external excitation. When the clearance decreases when the 0.3mm amplitude increased sharply as the Figure12, corresponding to the hinge and the dynamic stiffness coefficient will increase, and the theoretical calculation is consistent with the trend. The theoretical calculation is in good agreement with the experiment.

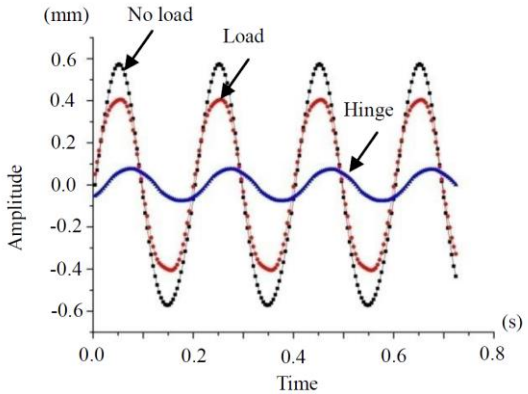

Figure 11. When the gap is 0.4mm, the hinge amplitude varies with the excitation

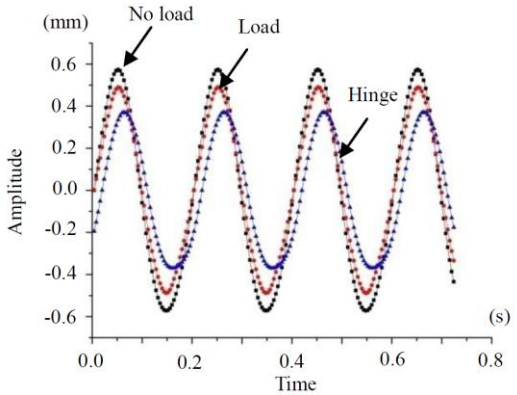

Figure 12. When the gap is 0.3mm, the hinge amplitude varies with the excitation

Apply a sweep excitation to the hinge, as shown in Figure13. The sweep frequency range is 1Hz-10Hz, the sweep time is 10s, and the clearance value is 0.4mm. The maximum amplitude of the external excitation is 0.604mm. In the initial stage, the input of 1Hz excitation, the amplitude of the hinge within a small range of shocks, when trigger sweep frequency, the amplitude of the hinge increases rapidly, thus it can be seen the excitation frequency promote the growth of the hinge amplitude, dynamic stiffness coefficient will decrease. Therefore, the external excitation increases the hinge dynamic stiffness coefficient and is consistent with the theoretical derivation.

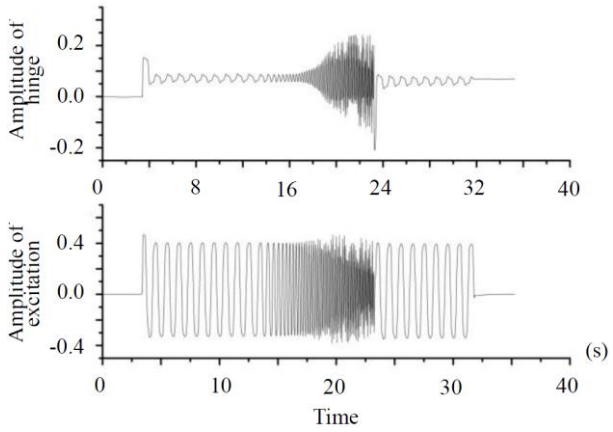

Figure 13. The amplitude variation of the hinge under swept frequency excitation

5. Conclusions

In this paper, the dynamic stiffness coefficient and damping of the clearance hinge structure in the large space deployable antenna ring truss structure under the radial motion are studied, the formulation of the radial clearance hinge dynamic expression of stiffness coefficient is carried out and verified by experiment, and meanwhile the damping characteristic is analysed. The size of the gap has a significant influence on the dynamic stiffness coefficient. When the gap is large, the dynamic stiffness coefficient increases obviously.

References

[1] Murphy D, McEachen M, Macy B, et al. *46th AIAA/ASME/ASCE/AHS/ASC Structures, Structural Dynamics and Materials Conference.* 2005: 2126.
[2] Chodimella S, Moore J, Otto J, et al. *47th AIAA/ASME/ASCE/AHS/ASC Structures, Structural Dynamics, and Materials Conference 14th AIAA/ASME/AHS Adaptive Structures Conference 7th.* 1916: 1603.
[3] Mitsugi J, Ando K, Senbokuya Y, et al. *ACTA ASTRONAUT*, 2000, 47(1): pp19-26.
[4] Tan G E B, Pellegrino S. Journal of Sound and Vibration, 2008, 314(3): pp783-802.
[5] Puig L, Barton A, Rando N. *ACTA ASTRONAUT*, 2010, 67(1): pp12-26.
[6] M.A. Brown. *Advances in Space Research*, 2011, 48(11): pp1747-1753.
[7] Moon F C, Li G X. *AIAA J*, 1990, 28(5): pp915-921.
[8] Bendiksen O O. *AIAA J*, 1987, 25(9): pp1241-1248.
[9] Hu H Y, Tian Q, Zhang W, et al. Advances in Mechanics, 2013, 43(4): pp390–414(in Chinese).
[10] Yoshida T. Journal of spacecraft and rockets, 2006, 43(4): pp771-779.
[11] Wang Y, Li F M. Applied Mathematical Modelling, 2015, 39(9): pp2518-2527.
[12] Lion C M. Journal of Vibration and Acoustics, 1991, pp113: 29.
[13] Wang J H, Liou C M. Journal of Sound and Vibration, 1990, 142(2): pp261-277.
[14] Crawley E F, Aubert A C. *AIAA J*, 1986, 24(1): pp155-162.
[15] Crawley E F, O'Donnel K J. *AIAA J*, 1987, 25(7): pp1003-1010.
[16] Ingham M D, Crawley E F. *AIAA J*, 2001, 39(2): pp331-338.
[17] Johnson K L. Contact mechanics. *Cambridge university press*, 1987.pp96-119.